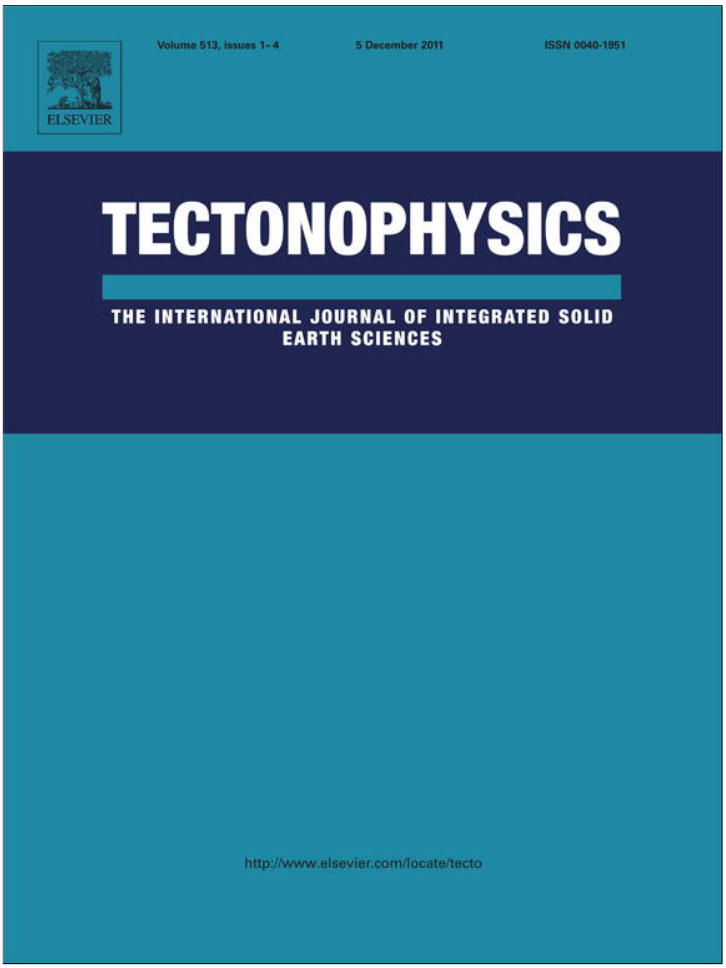

Tectonophysics 513 (2011) 49–53

Contents lists available at SciVerse ScienceDirect

Tectonophysics

journal homepage: www.elsevier.com/locate/tecto

The change of the entropy in natural time under time-reversal in the Olami–Feder–Christensen earthquake model

N.V. Sarlis, E.S. Skordas, P.A. Varotsos *

Solid State Section and Solid Earth Physics Institute, Physics Department, University of Athens, Panepistimiopolis, Zografos 157 84, Athens, Greece

ARTICLE INFO

Article history:
Received 19 April 2011
Received in revised form 14 September 2011
Accepted 30 September 2011
Available online 10 October 2011

Keywords:
Natural time
Olami–Feder–Christensen model
Entropy
Earthquakes
Self-organized
Criticality

ABSTRACT

Here, we analyze the Olami–Feder–Christensen (OFC) model for earthquakes in a new time domain, termed natural time χ. We show that there exists a non-zero change ΔS of the entropy in natural time upon time reversal. This reveals a breaking of the time symmetry, thus reflecting the predictability in the OFC model.

1. Introduction

The self-organized criticality (SOC) concept has been originally introduced by (Bak et al., 1987) using as an example the sandpile model. The fact that avalanches seem to be uncorrelated in the original sandpile model, has been used as an argument that is not possible to predict the occurrence of large avalanches, e.g., relevant claims are cited in Ramos et al. (2006, 2009). In other words, a belief has been expressed that power-law distributed avalanches are inherently unpredictable, which came from the concept of SOC, but interpreted in the way that, at any moment, any small avalanche can eventually cascade to a large event. However, prediction is in principle possible, as it became clear from the accumulated theoretical and experimental evidence (for a review see (Varotsos et al., 2011)). For example, the prediction of extreme avalanches in self-organized critical sandpiles has been studied in recent detailed numerical studies (Garber and Kantz, 2009; Garber et al., 2009) which showed that particularly large events in a close to SOC system can be predicted on the basis of past observations.

An important contribution to SOC ideas is the Olami–Feder–Christensen (OFC) earthquake model (Olami et al., 1992) which is probably (Ramos et al., 2006) the most studied non-conservative, supposedly, SOC model. It originated by a simplification of the Burridge–Knopoff (BK) spring-block model (Burridge and Knopoff, 1967) by mapping it into a non-conservative cellular automaton simulating the earthquake's behavior and introducing dissipation in the family of SOC systems. In the OFC model the force on a block is stored in a site of a square lattice, and the static friction threshold is assumed to have the same value over all blocks.

The criticality of the OFC model has been debated (e.g., (de Carvalho and Prado, 2000; Miller and Boulter, 2002)). Also, the SOC behavior of the model is destroyed upon introducing some small changes in the rules of the model, e.g., replacing open boundary conditions with periodic boundary conditions (Pérez et al., 1996), introducing frozen noise in the local degree of dissipation (Mousseau, 1996) or in its threshold value (Jánosi and Kertész, 1993), including lattice defects (Ceva, 1995) – which should not be confused with the intrinsic lattice defects in solids (Varotsos, 2007), e.g., Schottky (Varotsos and Alexopoulos, 1979, 1984a) or Frenkel (Varotsos, 1976; Varotsos and Alexopoulos, 1978) defects. Despite these findings as well as others which show (Peixoto and Davidsen, 2008), that it is insufficient to account for certain aspects of the *spatiotemporal* clustering of seismicity, the OFC model appears to show many features found in real earthquakes. As far as earthquake predictability (Pepke and Carlson, 1994) or Omori's law (Helmstetter et al., 2004; Hergarten and Neugebauer, 2002) is concerned, the OFC models appear to be closer to reality than others (Wissel and Drossel, 2006).

It has been shown (Abe et al., 2005) that the analysis of time series of complex systems in a new time domain, termed natural time χ (Varotsos et al., 2001, 2002, 2011), reduces uncertainty and extracts signal information as much as possible. Natural time analysis (recapitulated in Section 2) enables the study of the dynamic evolution of a complex system and identifies when the system approaches the critical point. Relevant applications of this new type of analysis with interesting results have been presented in a variety of cases including

* Corresponding author. Tel.: +30 210 9617573; fax: +30 210 9601721.
E-mail address: pvaro@otenet.gr (P.A. Varotsos).

0040-1951/$ – see front matter © 2011 Elsevier B.V. All rights reserved.
doi:10.1016/j.tecto.2011.09.025

seismicity (Sarlis et al., 2008, 2009, 2010; Varotsos et al., 2001, 2006a,2006b, 2008, 2011), identification (Varotsos et al., 2002, 2011) of the preseismic low frequency (≤1 Hz) variations of the electric field of the earth – termed Seismic Electric Signals (Varotsos and Alexopoulos, 1984b; Varotsos and Lazaridou, 1991; Varotsos et al., 1993) (SES) – that are emitted from the focal area when the stress reaches a critical value (Varotsos and Alexopoulos, 1984b; Varotsos et al., 1993, 2011) and precede earthquakes, e.g. for some recent examples see Uyeda and Kamogawa (2008, 2010) and Uyeda et al. (2009).

It is the main scope of this paper to show, on the basis of natural time analysis of the avalanche time series, the predictability of the OFC model whose summary is given in Section 3. To achieve this aim, we shall use recent complexity measures based on natural time, like the change ΔS of the entropy in natural time under time reversal as discussed in Section 4. These measures have been recently found to exhibit noticeable variations when approaching the critical point in a variety of complex systems. For example, we mention that when analyzing electrocardiograms in natural time, e.g. see (Varotsos et al., 2005a), we find (Varotsos et al., 2007) that: (a) The measure ΔS_l at the scale $l=3$ heartbeats, identifies the sudden cardiac death risk and distinguishes sudden cardiac death individuals from truly healthy individuals as well as from those with the life-threatening congestive heart failure. (b) Among those classified as sudden cardiac death individuals, the measured ΔS_l at the scale $l=13$ heartbeats provides an estimate of the occurrence time of the impending risk. The main conclusion is given in Section 5.

2. Natural time analysis. Background

Let us consider a time-series comprising N events. For example, in the case of SES activity – which is usually a time series of dichotomous nature – each event is a pulse of given duration Q, whereas for seismicity an earthquake of magnitude m. For a time-series of avalanches each event is an avalanche of size s. The *natural time* $\chi_k=k/N$ serves as an index (Varotsos et al., 2001, 2002) for the occurrence of the k-th event. In natural time analysis, the evolution of the pair (χ_k,E_k) is considered (Varotsos et al., 2001, 2002, 2006a, 2006b), where E_k denotes the energy released during the k-th event. This energy is itself proportional to the duration Q_k of each electric pulse in the case of SES activities, whereas for seismicity it is proportional to the seismic moment M_0, which is related (Kanamori, 1978) to the magnitude m through $M_0 \propto 10^{1.5m}$.

The evolution of either a SES activity or a series of earthquakes in natural time, can be analyzed as follows: For a SES activity, we consider the evolution (χ_k,Q_k), and define the continuous function $\Pi(\omega)$:

$$\Pi(\omega) = |\Phi(\omega)|^2 = \left| \sum_{k=1}^{N} p_k exp\left(i\omega \frac{k}{N}\right) \right|^2, \quad (1)$$

where $p_k = Q_k / \sum_{j=1}^{N} Q_j$, and $\omega = 2\pi\phi$, ϕ the natural frequency. For a seismic activity, we consider the evolution $(\chi_k, (M_0)_k)$, i.e., by ascribing to the k-th event, instead of Q_k, the corresponding seismic moment $(M_0)_k$. The continuous function $\Phi(\omega)$ is then defined by Eq. (1) with $p_k = (M_0)_k / \sum_{j=1}^{N} (M_0)_j$, for seismic events. Note, that in both cases, $\Pi(\omega)$ is a normalized power spectrum (Varotsos et al., 2001, 2002) that describes the process in natural time.

We focus on the properties of $\Pi(\omega)$ or $\Pi(\phi)$ for natural frequencies ϕ less than 0.5, since in this range of ϕ, $\Phi(\omega)$ or $\Phi(\phi)$ reduces (Varotsos et al., 2001, 2002, 2011) to a *characteristic function* for the probability distribution p_k in the context of probability theory. According to the probability theory, the moments of a distribution and hence the distribution itself can be approximately determined once the behavior of the characteristic function of the distribution is known around zero. For $\omega \to 0$, a Taylor expansion of Eq.(1) reveals that $\Pi(\omega) \approx 1 - \kappa_1 \omega^2$ where κ_1 is the variance of χ given by $\kappa_1 = \langle \chi^2 \rangle - \langle \chi^2 \rangle$, where $f(\chi) = \sum_{k=1}^{N} p_k f(\chi_k)$.

The entropy S in natural time is defined (Varotsos et al., 2011) as $S = \langle \chi ln \chi \rangle - \langle \chi \rangle ln \langle \chi \rangle$. It is *dynamic* entropy depending on the *sequential* order of pulses, e.g., see (Varotsos et al., 2005a, 2008). The entropy obtained upon considering (Varotsos et al., 2005b) the time reversal is labeled by S_-. The time reversal T is defined by $Tp_m = p_{N-m+1}$, which means that the last event becomes first, the last but one becomes second etc. It was found (Varotsos et al., 2005b) that, in general, S_- is different from S, and hence S shows the breaking of the time-reversal symmetry. We note that when considering a small increasing trend $\varepsilon(>0)$ for p_k versus k, via the parametric family (Varotsos et al., 2006b, 2008)

$$p(\chi;\varepsilon) \equiv 1 + \varepsilon(\chi - 1/2), \quad (2)$$

so that the corresponding entropy in natural time is given by

$$S(\varepsilon) \equiv \int_0^1 p(\chi;\varepsilon)\chi ln \chi d\chi - \left[\int_0^1 p(\chi;\varepsilon)\chi d\chi\right] ln \left[\int_0^1 p(\chi;\varepsilon)\chi d\chi\right], \quad (3)$$

we find (Varotsos et al., 2006b, 2008)

$$S(\varepsilon) = -\frac{1}{4} + \frac{\varepsilon}{72} - \left(\frac{1}{2} + \frac{\varepsilon}{12}\right) ln \left(\frac{1}{2} + \frac{\varepsilon}{12}\right). \quad (4)$$

Expanding Eq. (4) around $\varepsilon = 0$, we obtain that

$$S(\varepsilon) = S_u + \left(\frac{6ln2 - 5}{72}\right)\varepsilon + O\left(\varepsilon^2\right), \quad (5)$$

where $S_u \equiv \frac{2ln2-1}{4} \approx 0.0966$ is the entropy of the "uniform" distribution (Varotsos et al., 2011), e.g., when E_k are independent and identically distributed random variables. Since $S_-(\varepsilon)$ simply equals $S(-\varepsilon)$, we obtain that

$$S_-(\varepsilon) - S(\varepsilon) = \left(\frac{5 - 6ln2}{36}\right)\varepsilon + O\left(\varepsilon^3\right), \quad (6)$$

thus reflecting that an *increasing* trend in $p(\chi;\varepsilon)$, i.e., $\varepsilon > 0$, corresponds to *positive* $S_-(\varepsilon) - S(\varepsilon)$. The difference $S_- - S$ will be hereafter labeled ΔS (cf. if we alternatively (Varotsos et al., 2007) use this symbol to denote the opposite quantity, i.e., $S - S_-$, obviously an increasing trend would correspond to negative $S - S_-$). The quantity ΔS may also have a subscript (ΔS_l) meaning that the calculation is made (for each S and S_-) at a scale l (= number of successive events). In such a procedure, a window of length l is sliding, each time by one event, through the whole time series. The entropies S and S_-, and there from their difference ΔS_l, are calculated for each event. Thus, we form a new time series consisting of successive ΔS_l values.

3. The Olami–Feder–Christensen (OFC) model

The OFC model runs as follows: we assign a continuous random variable $z_{ij} \in (0,1)$ to each site of a square lattice, which represents the local 'energy'. Starting with a random initial configuration taken from a uniform distribution in the segment (0,1), the value z_{ij} of all sites is simultaneously increased at a uniform loading rate until a site ij reaches the threshold value $z_{thres} = 1$ (i.e., the loading Δf is such that $(z_{ij})_{max} + \Delta f = 1$). This site then topples which means that z_{ij} is reset to zero and an 'energy' αz_{ij} is passed to every nearest neighbor. If this causes a neighbor to exceed the threshold, the neighbor topples also, and the avalanche continues until all $z_{kl} < 1$. Then the uniform loading increase resumes. *The number of topplings defines the size s of an avalanche or "earthquake"*. This is the quantity that is used as the energy E_k in natural time analysis (Varotsos et al., 2011).

The coupling parameter α can take values from zero to 0.25. Smaller α means more dissipation, and $\alpha = 0.25$ corresponds to the conservative

case. The parameter α is the *only* parameter of the model, apart from the system size L, the edge length of the square lattice. Except from the initial condition the model is deterministic. The model can be supplemented by open boundary conditions in which the sites at the boundary distribute energy to the outer sites, which cannot topple, thus energy is removed at the boundary. Another possibility, is to use free boundary conditions: In this case, α varies locally

$$\alpha_{ij} = \frac{1}{n_{ij} + K} \tag{7}$$

where n_{ij} is the actual number of nearest neighbors of the site ij. For sites in the bulk $n_{ij}=4$, for sites at the edges $n_{ij}=3$ and for the four sites at the corners $n_{ij}=2$. The symbol K denotes the elastic constant of the upper leaf springs measured relatively to that of the other springs between blocks (Helmstetter et al., 2004) in the BK model. Obviously the OFC model is non-conservative for $K>0$ for which $\alpha_{ij}<0.25$ in the bulk. Finally, periodic boundary conditions (PBC) can be imposed but these destroy (Pérez et al., 1996) criticality.

Concerning the study of the transient regime of the OFC model, it can be simplified (Varotsos et al., 2011) when done in terms of the quantity $f=\sum(\Delta f)$, which represents the total increase of z_{ij} due to the external force loading in each site. Since the loading rate is assumed uniform in time, f plays a role analogous to that of the conventional time $T\equiv f$. de Carvalho and Prado (2003) found that the conservative and non-conservative cases display a qualitatively different behavior. This has been also verified by natural time analysis (Varotsos et al., 2011). Here, in what follows, we shall solely focus on the stationary regime of the OFC model.

4. The predictability of the OFC model using the entropy change ΔS under time reversal

We first mention that the predictability of the OFC model, for which the presence of 'foreshocks' (as well as 'aftershocks') has been identified by Hergarten and Neugebauer (2002) in the non-conservative case, has been studied by Pepke and Carlson (1994) and Pepke et al. (1994). Recently Caruso and Kantz (2011) have provided an efficient algorithm for the prediction of large avalanches solely based on the past avalanches for the non-conservative OFC model on a small world topology. Moreover, Varotsos et al. (2011) have shown that if we consider the mean 'energy' per site $\zeta=\sum z_{ij}/L^2$ which is a function of the 'time' T, as a decision variable such a goal is possible even for the OFC model on a square lattice. Here, we focus our interest on the entropy change ΔS in natural time before large avalanches in the original OFC model on a square lattice and show that ΔS may provide a decision variable for the prediction of a large avalanche in the next natural time step.

The occurrence of 'foreshocks' as well as 'aftershocks' in the OFC model has been exhaustively studied by Helmstetter et al. (2004). Here, we solely focus on the former (foreshocks) that are described by the so-called inverse Omori's law (Helmstetter et al., 2003, 2004) which states that the average increase of seismicity observed at the time t before the occurrence time t_c of a mainshock is given by

$$N_f(t) = \frac{K_f}{(t_c - t + c)^{p_f}} \tag{8}$$

where the subscript "f" refers to the foreshocks and the quantities K_f and c are taken constants. The inverse Omori's exponent p_f is usually close to or slightly *smaller* than the corresponding (Helmstetter and Sornette, 2003) exponent p_a of the usual Omori's law for aftershocks. Helmstetter et al. (2004) defined "mainshock" (see their definition $d=0$) as any earthquake of magnitude m which was not preceded or followed by a larger earthquake in a time window of length $T(m)$ equal to 1% of the average return time of an earthquake of magnitude m. Foreshocks are then selected as all earthquakes occurring within the time $T(m)$ before a mainshock. The value of p_f has been found by averaging the seismicity rate before a large number of mainshocks (Helmstetter and Sornette, 2003), because there are huge fluctuations of the rate of seismicity before individual mainshocks. Thus, following the method of study of foreshocks in Helmstetter et al. (2004), our results for ΔS are found by averaging the values obtained before an appreciably high number of large avalanches.

Assuming that the large avalanche occurs at T_0, Fig. 1 depicts the results for the average change ΔS (left scale) of the entropy in natural time under time reversal and the average value of the mean 'energy' ζ (right scale) obtained by using the last 500 avalanches (irrespective of their size) before a large avalanche of size $s\geq 100$ (red), 500 (green) and 700 (blue) in the non-conservative OFC model with $L=64$ and $K=2$. They have been obtained by analyzing 10^7 avalanches after the system has reached the steady SOC state. In the horizontal axis, the time is measured from the occurrence time T_0 of the large avalanche. We find that the magnitude of ΔS_l maximizes before the impending large avalanche, thus signaling the imminent major event. The positive values of ΔS reflect, through Eq. (6), that the avalanche size tends to increase as the time approaches that of the mainshock (cf. due to the foreshocks, mentioned above, that start to become discernable from the background seismicity). The decrease of ΔS that occurs after a maximum at $T_0-T\approx 0.15$ before the mainshock, reflects that the 'effective' trend ε, which was defined in natural time (see Eq. (2)), should simultaneously decrease. This appears so, because it is the relative intensity of the events that is considered (through $p_k = E_k/\sum_{j=1}^{N} E_j$) in the calculations in natural time. Using Eq. (8) and taking as a measure of the 'effective' trend the ratio of p_N which corresponds to the last event (i.e., the foreshock that occurred just before the mainshock at time t_{-1}) over p_1, we obtain that

$$\frac{p_N}{p_1} = \left(\frac{t_c - t_i + c}{t_c - t_{-1} + c}\right)^{p_f}, \tag{9}$$

where t_i denotes the time of occurrence of the initial foreshock taken into account in the natural time entropy calculation. As t_i approaches t_{-1}, Eq.(9) results in smaller values of p_N/p_1, thus reflecting a decreasing effective trend ε. In fact, Fig. 1 shows that the average entropy change in natural time becomes zero when $T_0-T\approx 0$ (in this case, Eq. (9) leads to an absence of trend since $p_N/p_1\to 1$ as $t_i\to t_{-1}$). Furthermore, note that ΔS changes sign, becoming positive, when the

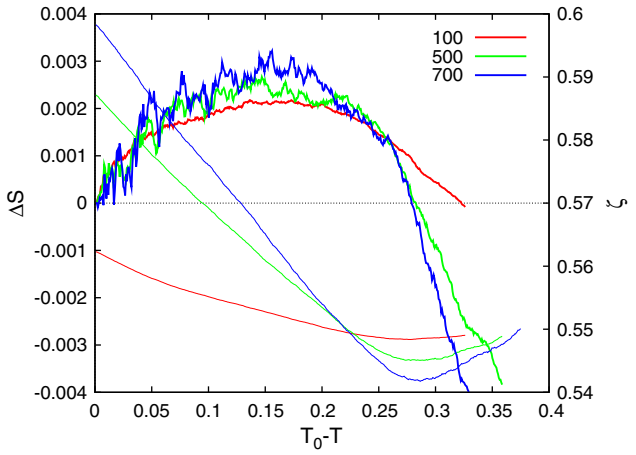

Fig. 1. Results from averaging the last 500 events before a large avalanche ($s\geq 100$, 500, 700 occurring at T_0) in the OFC model with $L=64$ and $K=2$: The change ΔS (left scale, thick lines) of the entropy in natural time under time reversal and the mean energy ζ (right scale, thin lines) as a function of the 'time' (T_0-T) to the large avalanche. Note that ΔS maximizes *before* the occurrence time T_0 of the large avalanche, and changes sign when ζ almost starts to increase.

parameter ζ almost starts to increase (cf. recall that the quantity ζ as mentioned can be used as a predictor for the large avalanches).

Proceeding one step further, we now examine whether the entropy change ΔS in natural time under time-reversal can be used for the prediction of a large avalanche in the next natural time step. For this reason, based on the results shown in Fig. 1, we determine the quantity $\bar{\Delta S}$ which is the average value of ΔS using the past events that occurred at time T within the period $\Delta T = T_{now} - T = 0.05$ to 0.2, where T_{now} stands for the present time. The quantity $\bar{\Delta S}$ can be considered as a decision variable in the sense that the time increased probability (TIP) is turned on when $\bar{\Delta S} > \bar{\Delta S}_c$, where $\bar{\Delta S}_c$ is a given threshold in the prediction. If the size s of the next avalanche is greater than a target avalanche size threshold s_c, we have a successful prediction. For binary predictions, the prediction of events becomes a classification task with two types of errors: missing an event and giving a false alarm. We therefore choose, following (Garber et al., 2009), the receiver operating characteristics (ROC) graph (Fawcett, 2006) to depict here the prediction quality. This is a plot of the hit rate versus the false alarm rate, as a function of the total rate of alarms, which here is tuned by the threshold $\bar{\Delta S}_c$. Only if in between the hit rate exceeds the false alarm rate, the predictor is useful. Random predictions generate equal hit and alarm rate, and hence they lead to the diagonal in the ROC plot. (If $\bar{\Delta S}_c$ is maximum, both hit rate and false alarm rate are zero, while for very small $\bar{\Delta S}_c$ values both rates tend to unity.) Thus, only when the points lie above this diagonal the predictor is useful. As an example, the ROC graph for $L = 64$ and $K = 2$ is shown in the inset of Fig. 2. For every given threshold value $\bar{\Delta S}_c$ and a target threshold s_c, we get a point in this plot, thus varying $\bar{\Delta S}_c$ we get a curve. The various curves in the middle of the inset of Fig. 2 correspond to various values of s_c increasing from the bottom to the top. Recalling that the diagonal line in such a plot corresponds to random predictions, and the points in each curve lie above it (meaningful prediction), we conclude that the precursory function $\bar{\Delta S}$ can be considered as a possible predictor. In order to investigate the statistical significance of the results as well as the reason behind the possible predictive power of $\bar{\Delta S}$, we insert in Fig. 2 the results obtained (blue curves) from 100 trials when performing the same calculation by using *randomly* shuffled $\bar{\Delta S}$ values. We observe that the results obtained for the original $\bar{\Delta S}$ time-series are well above those obtained even from the extreme of 100 trials using *randomly* shuffled $\bar{\Delta S}$ values. Thus, the predictions made on the basis of $\bar{\Delta S}$ are statistically significant, and as concerns the origin of their predictive power it should be attributed to the fact that ΔS is able to catch the 'true' time arrow as mentioned.

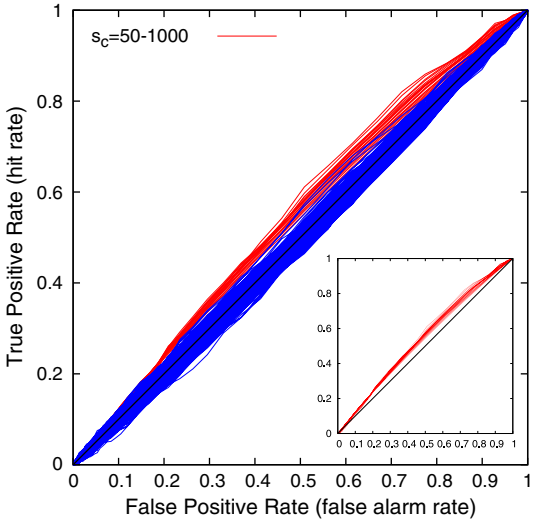

Fig. 2. Receiver operating characteristics graph (red) for the OFC model with $L = 64$ and $K = 2$ when using $\bar{\Delta S}$ as a predictor: The true positive rate (hit rate) versus the false positive rate (false alarm rate) for various values of the target avalanche size threshold $s_c = 50, 100, 150, \ldots 1000$. At false alarm rate equal to 50% the lower curve corresponds to $s_c = 50$ and the upper one to $s_c = 1000$. The blue curves depict the results obtained when repeating 100 times the same calculation using *randomly* shuffled $\bar{\Delta S}$ values as a predictor. The inset reproduces the red curves for the sake of clarity.

5. Conclusion

The natural time analysis of the avalanches in the stationary regime of the OFC model reveals that that there is a non-zero change ΔS of the entropy S in natural time under time-reversal. This signals the breaking of the time symmetry, thus reflecting predictability in the OFC model.

References

Abe, S., Sarlis, N.V., Skordas, E.S., Tanaka, H.K., Varotsos, P.A., 2005. Origin of the usefulness of the natural-time representation of complex time series. Physical Review Letters 94, 170601.

Bak, P., Tang, C., Wiesenfeld, K., 1987. Self-organized criticality: an explanation of the 1/f noise. Physical Review Letters 59, 381–384.

Burridge, R., Knopoff, L., 1967. Model and theoretical seismicity. Bulletin of the Seismological Society of America 57, 341–371.

Caruso, F., Kantz, H., 2011. Prediction of extreme events in the OFC model on a small world network. European Physical Journal B 79, 7–11.

de Carvalho, J.X., Prado, C.P.C., 2000. Self-organized criticality in the Olami–Feder–Christensen model. Physical Review Letters 84, 4006–4009.

de Carvalho, J.X., Prado, C.P.C., 2003. Dealing with transients in models with self-organized criticality. Physica A: Statistical Mechanics and its Applications 321, 519–528.

Ceva, H., 1995. Influence of defects in a coupled map lattice modeling earthquakes. Physical Review E 52, 154–158.

Fawcett, T., 2006. An introduction to ROC analysis. Pattern Recognition Letters 27, 861–874.

Garber, A., Hallerberg, S., Kantz, H., 2009. Predicting extreme avalanches in self-organized critical sandpiles. Physical Review E 80, 026124.

Garber, A., Kantz, H., 2009. Finite-size effects on the statistics of extreme events in the BTW model. European Physical Journal B 67, 437–443.

Helmstetter, A., Hergarten, S., Sornette, D., 2004. Properties of foreshocks and aftershocks of the nonconservative self-organized critical Olami–Feder–Christensen model. Physical Review E 70, 046120.

Helmstetter, A., Sornette, D., 2003. Foreshocks explained by cascades of triggered seismicity. Journal of Geophysical Research 108, 2457.

Helmstetter, A., Sornette, D., Grasso, J.R., 2003. Mainshocks are aftershocks of conditional foreshocks: how do foreshock statistical properties emerge from aftershock laws. Journal of Geophysical Research 108, 2046.

Hergarten, S., Neugebauer, H.J., 2002. Foreshocks and aftershocks in the Olami–Feder–Christensen model. Physical Review Letters 88, 238501.

Jánosi, I., Kertész, J., 1993. Self-organized criticality with and without conservation. Physica A 200, 179–188.

Kanamori, H., 1978. Quantification of earthquakes. Nature 271, 411–414.

Miller, G., Boulter, C.J., 2002. Measurements of criticality in the Olami–Feder–Christensen model. Physical Review E 66, 016123.

Mousseau, N., 1996. Synchronization by disorder in coupled systems. Physical Review Letters 77, 968–971.

Olami, Z., Feder, H.J.S., Christensen, K., 1992. Self-organized criticality in a continuous, non-conservative cellular automaton modeling earthquakes. Physical Review Letters 68, 1244–1247.

Peixoto, T.P., Davidsen, J., 2008. Network of recurrent events for the Olami–Feder–Christensen model. Physical Review E 77, 066107.

Pepke, S.L., Carlson, J.M., 1994. Predictability of self-organizing systems. Physical Review E 50, 236–242.

Pepke, S.L., Carlson, J.M., Shaw, B.E., 1994. Prediction of large events on a dynamical model of a fault. Journal of Geophysical Research 99, 6769–6788.

Pérez, C.J., Corral, A., Díaz-Guilera, A., Christensen, K., Arenas, A., 1996. On self-organized criticality and synchronization in lattice models of coupled dynamical systems. International Journal of Modern Physics B 10, 1111.

Ramos, O., Altshuler, E., Måløy, K.J., 2006. Quasiperiodic events in an earthquake model. Physical Review Letters 96, 098501.

Ramos, O., Altshuler, E., Måløy, K.J., 2009. Avalanche prediction in a self-organized pile of beads. Physical Review Letters 102, 078701.

Sarlis, N.V., Skordas, E.S., Lazaridou, M.S., Varotsos, P.A., 2008. Investigation of seismicity after the initiation of a seismic electric signal activity until the main shock. Proceedings of the Japan Academy Series B, Physical and Biological Sciences 84, 331–343.

Sarlis, N.V., Skordas, E.S., Varotsos, P.A., 2009. Multiplicative cascades and seismicity in natural time. Physical Review E 80, 022102.

Sarlis, N.V., Skordas, E.S., Varotsos, P.A., 2010. Order parameter fluctuations of seismicity in natural time before and after mainshocks. EPL 91, 59001.

Uyeda, S., Kamogawa, M., 2008. The prediction of two large earthquakes in Greece. EOS, Transactions, American Geophysical Union 89, 363.
Uyeda, S., Kamogawa, M., 2010. Comment on 'the prediction of two large earthquakes in Greece'. EOS, Transactions, American Geophysical Union 91, 163.
Uyeda, S., Kamogawa, M., Tanaka, H., 2009. Analysis of electrical activity and seismicity in the natural time domain for the volcanic-seismic swarm activity in 2000 in the Izu island region, Japan. Journal of Geophysical Research 114, B02310. doi:10.1029/2007JB005332.
Varotsos, P., 1976. Comments on the formation entropy of a Frenkel defect in BaF_2 and CaF_2. Physical Review B 13, 938.
Varotsos, P., 2007. Comparison of models that interconnect point defect parameters in solids with bulk properties. Journal of Applied Physics 101, 123503.
Varotsos, P., Alexopoulos, K., 1978. The curvature in conductivity plots of silver halides as a consequence of anharmonicity. Journal of Physics and Chemistry of Solids 39, 759–761.
Varotsos, P., Alexopoulos, K., 1979. On the possibility of the enthalpy of a Schottky defect decreasing with increasing temperature. Journal of Physics C: Solid State 12, L761–L764.
Varotsos, P., Alexopoulos, K., 1984a. Connection between the formation volume and formation Gibbs energy in noble-gas solids. Physical Review B 30, 7305–7306.
Varotsos, P., Alexopoulos, K., 1984b. Physical properties of the variations of the electric field of the Earth preceding earthquakes. Tectonophysics 110, 73–98 110, 99–125.
Varotsos, P., Alexopoulos, K., Lazaridou, M., 1993. Latest aspects of earthquake prediction in Greece based on seismic electric signals, II. Tectonophysics 224, 1–37.
Varotsos, P., Lazaridou, M., 1991. Latest aspects of earthquake prediction in Greece based on seismic electric signals. Tectonophysics 188, 321–347.
Varotsos, P., Sarlis, N., Skordas, E., 2011. Natural time analysis: the new view of time. Precursory Seismic Electric Signals, Earthquakes and other Complex Time-Series. Springer-Verlag, Berlin Heidelberg.
Varotsos, P.A., Sarlis, N.V., Skordas, E.S., 2001. Spatio-temporal complexity aspects on the interrelation between seismic electric signals and seismicity. Practica of Athens Academy 76, 294–321.
Varotsos, P.A., Sarlis, N.V., Skordas, E.S., 2002. Long-range correlations in the electric signals the precede rupture. Physical Review E 66, 011902.
Varotsos, P.A., Sarlis, N.V., Skordas, E.S., Lazaridou, M.S., 2005a. Natural entropy fluctuations discriminate similar-looking electric signals emitted from systems of different dynamics. Physical Review E 71, 011110.
Varotsos, P.A., Sarlis, N.V., Skordas, E.S., Lazaridou, M.S., 2007. Identifying sudden cardiac death risk and specifying its occurrence time by analyzing electrocardiograms in natural time. Applied Physics Letters 91, 064106.
Varotsos, P.A., Sarlis, N.V., Skordas, E.S., Lazaridou, M.S., 2008. The fluctuations, under time reversal, of the natural time and the entropy distinguish similar looking electric signals of different dynamics. Journal of Applied Physics 103, 014906.
Varotsos, P.A., Sarlis, N.V., Skordas, E.S., Tanaka, H.K., Lazaridou, M.S., 2006a. Attempt to distinguish long-range temporal correlations from the statistics of the increments by natural time analysis. Physical Review E 74, 021123.
Varotsos, P.A., Sarlis, N.V., Skordas, E.S., Tanaka, H.K., Lazaridou, M.S., 2006b. Entropy of seismic electric signals: Analysis in the natural time under time reversal. Physical Review E 73, 031114.
Varotsos, P.A., Sarlis, N.V., Tanaka, H.K., Skordas, E.S., 2005b. Some properties of the entropy in the natural time. Physical Review E 71, 032102.
Wissel, F., Drossel, B., 2006. Transient and stationary behavior of the Olami–Feder–Christensen model. Physical Review E 74, 066109.